

Soil salinity mapping using remote sensing and GIS

Mahmoud Mohamed El-Sayed Gad, Mostafa H.A. Mohamed, and Mervat Refaat Mohamed

Abstract: The monitoring of soil salinity plays a vital role in agricultural society. Soil salinity causes land degradation processes, especially in arid and semi-arid regions, which influence soil properties, reduce yield production of crops, and affect infrastructure. This research produces soil salinity mapping of the East Delta in Egypt in 1995 using remote sensing technology. A Landsat 5 image taken on 26 September 1995 was used. Radiometric and atmospheric corrections for satellite data were applied. Different salinity indices (SIs) were used, such as the normalized difference salinity index, SI1, SI2, SI3, SI4, SI5, SI6, and SI7, in addition to the normalized difference vegetation index, which was used for data filtration. The field's electrical conductivity was measured during the period from 22 to 26 September 1995 by the Japanese International Cooperation Agency. These data were used as ground truth for the correlation analysis with different indices image bands values. Simple linear regression and mean relative error were used to find the best index, which was SI5 with a 0.87 correlation with field truth data and mean relative error equal 22.7%. This index was used to produce a salinity map of the Eastern Delta with acceptable accuracy. Finally, it is concluded that using remote sensing in salinity detection and mapping is highly appreciated.

Key words: soil salinity, electrical conductivity, digital number, indices of salinity, GIS, remote sensing.

Résumé : La surveillance de la salinité des sols joue un rôle essentiel dans la société agricole. La salinité du sol entraîne des processus de dégradation des terres, en particulier dans les régions arides et semi-arides, qui influencent les propriétés du sol, réduisent le rendement des cultures et affectent les infrastructures. Cette recherche produit une cartographie de la salinité du sol du Delta oriental en Égypte en 1995 en utilisant la technologie de la télédétection. L'image Landsat 5 prise le 26 septembre 1995 a été utilisée. Les corrections radiométriques et atmosphériques des données satellitaires ont été appliquées. Différents indices de salinité (IS) ont été utilisés tels que l'indice de salinité par différence normalisée, IS1, IS2, IS3, IS4, IS5, IS6 et IS7, ainsi que l'indice de végétation par différence normalisée qui a été utilisé pour le filtrage des données. La conductivité électrique du champ a été mesurée entre le 22 et le 26 septembre 1995 par l'Agence japonaise de coopération internationale. Ces données ont été utilisées comme vérité de base pour l'analyse de corrélation avec les valeurs des différentes bandes d'images d'indices. La régression linéaire simple et l'erreur relative moyenne ont été utilisées pour trouver le meilleur indice qui était IS5 avec une corrélation de 0,87 avec les données de vérité sur le terrain

Received 7 October 2021. Accepted 20 October 2022.

M.M.E.-S. Gad. Canadian International College, Cairo, Egypt.

M.H.A. Mohamed. Faculty of Engineering, Al-Azhar University, Cairo, Egypt.

M.R. Mohamed. Benha University, Egypt Head of Civil Engineering Department, Canadian International College, Cairo, Egypt.

Corresponding author: Mahmoud Mohamed El-Sayed Gad (email: mahmoud.gad2691@gmail.com).

© 2022 The Author(s). This work is licensed under a [Creative Commons Attribution 4.0 International License](https://creativecommons.org/licenses/by/4.0/) (CC BY 4.0), which permits unrestricted use, distribution, and reproduction in any medium, provided the original author(s) and source are credited.

et une erreur relative moyenne égale à 22,7%. Cet indice a été utilisé pour produire une carte de salinité du delta oriental avec une précision acceptable. Enfin, il est conclu que l'utilisation de la télédétection dans la détection et la cartographie de la salinité est très appréciée. [Traduit par la Rédaction]

Mots-clés : salinité du sol, conductivité électrique, nombre numérique, indices de salinité, SIG, télédétection.

1. Introduction

Soil salinization is increasing all over the world and is spreading in over 100 countries (Shahid et al. 2013). In Egypt, the northern parts of the Nile Delta are suffering from increasing salinization of soils and the groundwater table where the climate causes an increase in salinity. The salinization of soils and groundwater in recent decades is a major agricultural problem in Egypt. It is thought to be a result of the Nile's weak demineralization of the soil due to the absence of flooding (Mohamed et al. 2011). Due to the increasing population in Egypt, it is important to study agricultural threats, and soil salinization is one of them. The salinization of soil occurs due the accumulation of salts in the soil, which is a worldwide environmental issue that affects adversely the growth of plants and crop production, especially in arid and semi-arid regions. It becomes worse and affects agricultural production and the utilization of land resources. Traditional methods for soil salinity measurements are expensive and time-consuming. The remote sensing technique has proved good and reliable in this concern (Asfaw et al. 2018). The salinity map of the specified area can be made by comparing laboratory measurements with satellite image values to find the best correlated salinity index (SI). Soil salinity can be expressed by electrical conductivity (EC), and that affects crops as shown in the agronomic classification of soil salinity as shown in Table 1 (Brown et al. 1954).

Soil that has an $EC > 4$ ds/m (decisiemens per meter) at 25 °C will be harmful to crops and will affect plant growth (Morshed et al. 2016). The use of remote sensing in the detection of soil salinity is widespread, and studies showed that using band ratios of visible to near infrared and between infrared bands have proven better in identifying salts in soils and salt-stressed crops (Schneider et al. 2010). Remote sensing is sensitive in soil salinity detection when the depth is shallow, as many other types of research achieved good correlation when the depth is less than 50 cm (Amal and Benni 2010; El-Dein Galal 2017; Tran et al. 2018; Hammam and Mohamed 2020; Metternicht 2008).

2. Study area and data

2.1. Description of the study area

The investigated area is located in Egypt in the east of the Nile Delta in the Al-Behira governorate. It is bounded geographically by longitudes 29°44'30"E and 29°51'30"E and latitudes 31°5'0"N and 31°10'0"N based on the Japanese International Cooperation Agency (JICA) report (Japan International Cooperation Agency 1995) as shown in Fig. 1.

The study area is characterized by arid and semi-arid climates during the surveying on 26 September 1996. The temperature was 28.4 °C, and the humidity was 47%. The average monthly temperature was 31.1 °C, the average monthly humidity was 35.2%, and there was no rainfall during that month. The soil texture varies from sand to clay, where the percentage of clay increases towards the middle of Nile Delta (Japan International Cooperation Agency 1995).

Table 1. Agronomic classification of soil salinity based on electrical conductivity (EC).

Classification	EC (ds/m)	Crop yield
Non-saline soils	0–2	Not affected
Slightly saline soils	2–4	Sensitive crop affected
Saline soils	4–8	Many crops affected
Strongly saline soils	8–16	Only tolerant crops possible
Extremely saline soils	>16	A few very tolerant crops possible

Figure 1. Study area of Al-Behira using ARCGIS, projected to WGS84 and UTM coordinate system. [Colour online.]

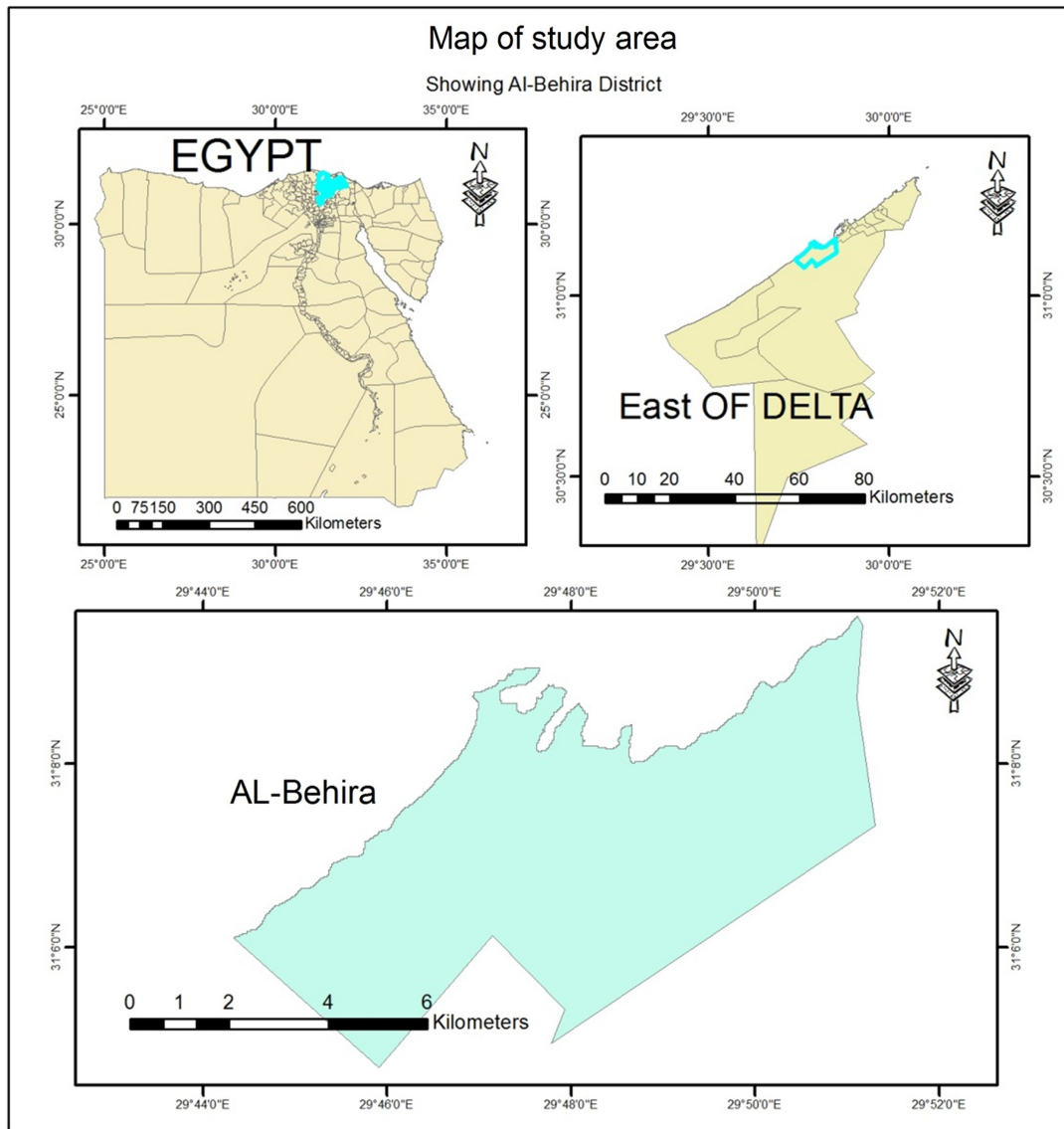


Figure 2. Locations of soil samples from the Japanese International Cooperation Agency (JICA) report using ARCGIS, projected to WGS84 and UTM coordinate system. [Colour online.]

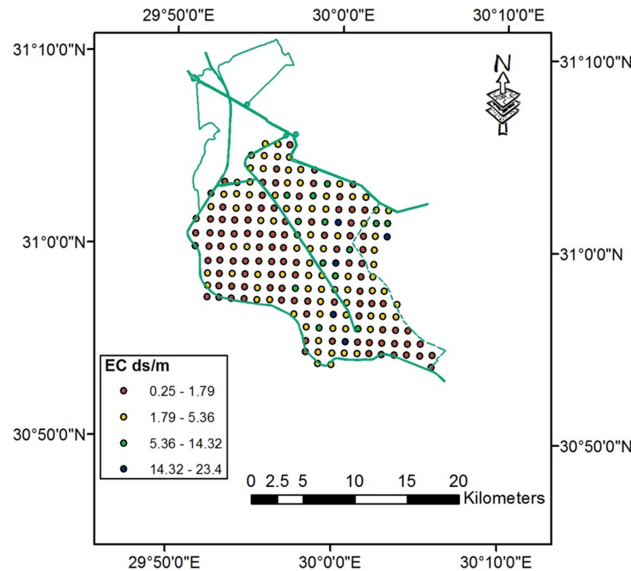


Table 2. Landsat 5 band specifications.

Bands	Wavelength (μm)	Spatial resolution (m)
Band 1 (Blue)	0.45–0.52	30
Band 2 (Green)	0.52–0.6	30
Band 3 (Red)	0.63–0.69	30
Band 4 (NIR)	0.76–0.9	30
Band 5 (SWIR-1)	1.55–1.75	30
Band 6 (Thermal)	10.4–12.5	120
Band 7 (SWIR-2)	2.08–2.35	30

2.2. Ground truth measurements

Fieldwork for soil salinity measurements was performed in September 1995 by JICA as part of the El-Omoum drainage improvement project, 200 surface soil samples at a depth of 0–50 cm. These soil samples were carried out in a systematic random method with a 1.2 km interval. Each sample covered approximately 144 hectares based on JICA studies. These augers locations were uniformly distributed throughout the study area describing physicochemical soil properties at each location as shown in Fig. 2.

Each sample was air dried, ground, sieved with a 2 mm sieve, and stored in a plastic bag until analysis. The soil samples were sent to the laboratory to measure the EC of the solution extracted from a saturated soil paste, as it is considered a standard and universally accepted way of measuring soil salinity (Bannari et al. 2017). The EC in this area varied from 0.25 to 23.4 ds/m.

2.3. Satellite data

A Landsat 5TM (thematic mapper) with band specifications shown in Table 2 was used as it was the available Landsat during the fieldwork period.

Figure 3. Study area Landsat reduced image from United States Geological Survey (USGS) website using ARCGIS, projected to WGS84 and UTM coordinate system. [Colour online.]



The image was rectified to the Universal Transverse Mercator (UTM) and the coordinate system World Geodetic System 1984 (WGS84) and assigned to north UTM zone 36, path 177, and row 39. The image on 26 September 1995 was downloaded from the United States Geological Survey website (<http://earthexplorer.usgs.gov/>). The image had clouds less than 10%, sun azimuth = 127.08° , and sun elevation = 44.40° as shown in Fig. 3.

3. Methodology

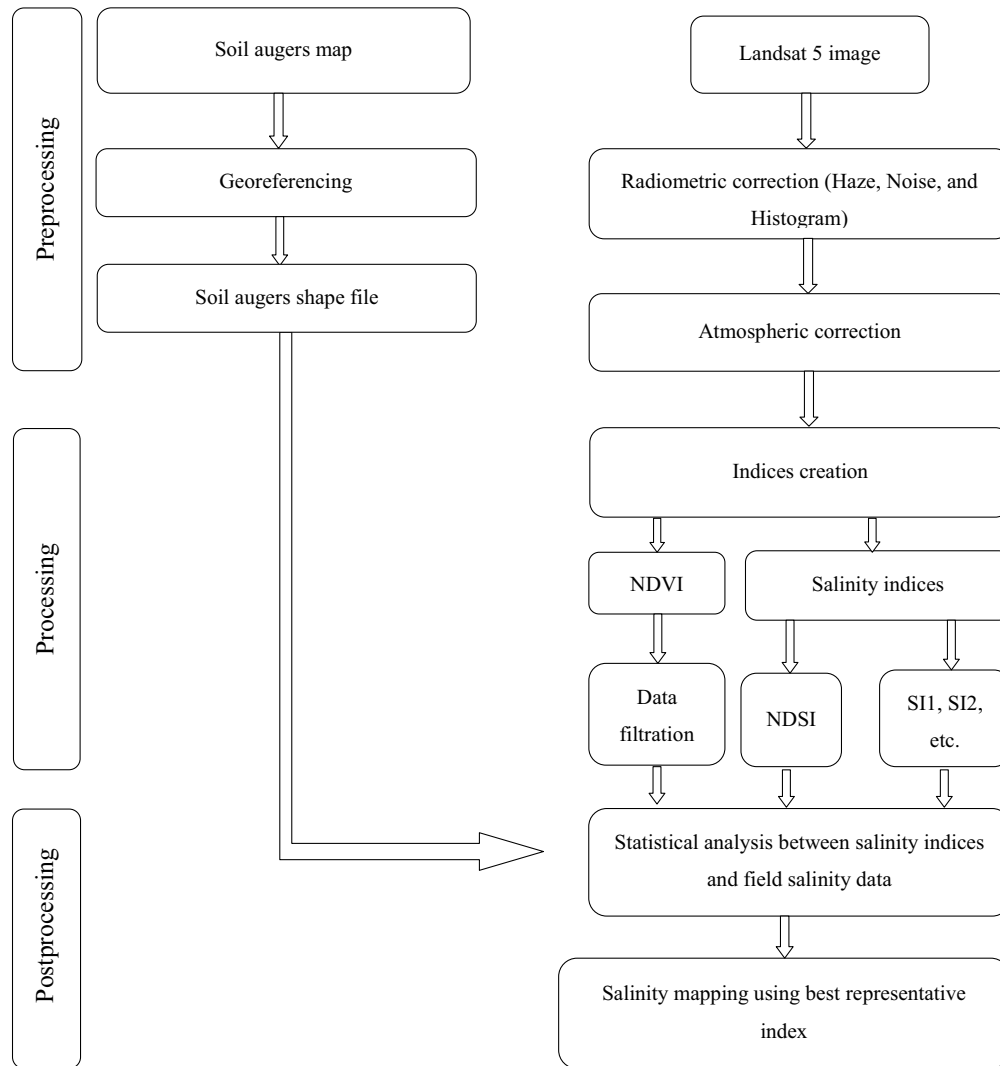
The methodology adopted in this research can be expressed in three main stages: (i) the preprocessing of both the augers map and the Landsat image, (ii) the processing of data, and (iii) the postprocessing, as shown in Fig. 4 and the following subsections.

3.1. Preprocessing of data (stage 1)

Step 1: Preprocessing of the soil augers map

Firstly, the soil augers map obtained from the JICA report of the El-Omoum project was imported to GIS software (ArcMap, Esri, Redlands, CA, USA) and defined to WGS84 datum and UTM Zone 36 North. The georeferencing was made using three control points: Max pump station $31^\circ 08' 39.4'' \text{N}$ $29^\circ 50' 58.7'' \text{E}$, Apis pump station $31^\circ 07' 45.3'' \text{N}$ $29^\circ 53' 06.5'' \text{E}$, and Dushoudi pump station $31^\circ 06' 04.0'' \text{N}$ $29^\circ 56' 33.6'' \text{E}$. A shape file was made for the augers and then exported to ERDAS IMAGINE software (Norcross, GA, USA) for image analysis.

Figure 4. Flowchart for adopted methodology procedures.



Step 2: Preprocessing of the Landsat image

The Landsat image downloaded required radiometric and atmospheric corrections as follows.

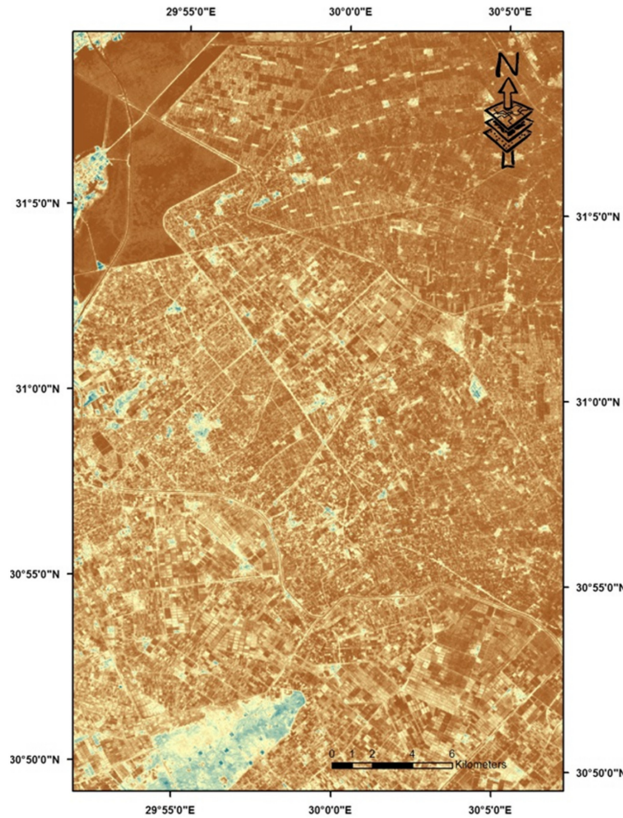
- Radiometric correction

The Landsat image must be radiometrically corrected to reduce the error of the digital number of the image. This was done with ERDAS IMAGINE software depending on the following processes for radiometric correction:

1. Haze reduction

The internet protocol module reduces damp haze and fog in images; it improves the readability and visibility in digital images (Ahmad et al. 2019).

Figure 5. Landsat image after radiometric and atmospheric corrections using ARCGIS, projected to WGS84 and UTM coordinate system. [Colour online.]



2. Noise reduction

Noise removal is a basic preprocessing step in Landsat data (Findings 2013). Noise is the pixels in the image that show different pixel value intensity instead of the true one obtained from the image. Noise removal is the step of removing or lowering the noise in the image. Noise removal is a basic preprocessing step in satellite images.

3. Histogram equalization

Histogram equalization is a procedure in the processing of images. Histogram equalization is the adjustment of contrast using the image's histogram. This method is used to increase the contrast of images.

After the radiometric correction, the obtained image was used for the atmospheric correction process.

- Atmospheric correction

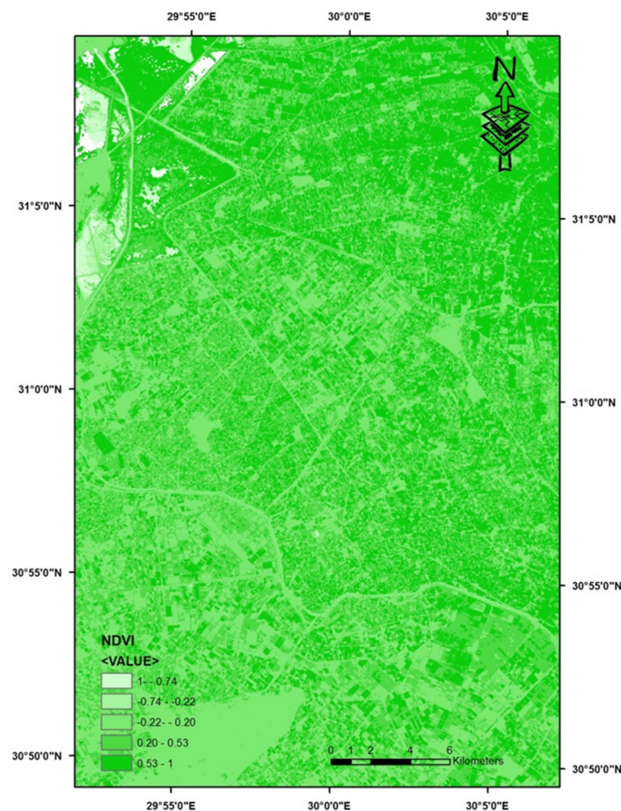
Atmospheric correction is the most important part of preprocessing of the Landsat images, as it aims to get the true reflectance of the surface by removing the atmosphere effect. This step was done using Atmospheric and Topographic Correction (ATCOR-3; German Aerospace Center, Cologne, Germany), which is highly recommended in atmospheric correction for remote sensing data (Fuyi et al. 2013). Finally, the obtained image that was used for processing is shown in Fig. 5.

Table 3. Spectral salinity indices.

Index	Reference
Normalized difference salinity index (NDSI) = $\frac{R - NIR}{R + NIR}$	Khan et al. 2001
Salinity index 1 (SI1) = $\sqrt{G} \times R$	Douaoui et al. 2006
Salinity index 2 (SI2) = $\sqrt{B} \times R$	Khan et al. 2001
Salinity index 3 (SI3) = $\frac{B-R}{B+R}$	Bannari et al. 2008
Salinity index 4 (SI4) = $\frac{NIR}{R}$	Major et al. 1990
Salinity index 5 (SI5) = $\frac{R \times NIR}{G}$	Abbas and Khan 2007
Salinity index 6 (SI6) = $\frac{B \times R}{G}$	Abbas and Khan 2007

Note: B, blue band; G, green band; NIR, near infrared band; R, red band.

Figure 6. Vegetation index image (NDVI image) using ARCGIS, projected to WGS84 and UTM coordinate system. [Colour online.]

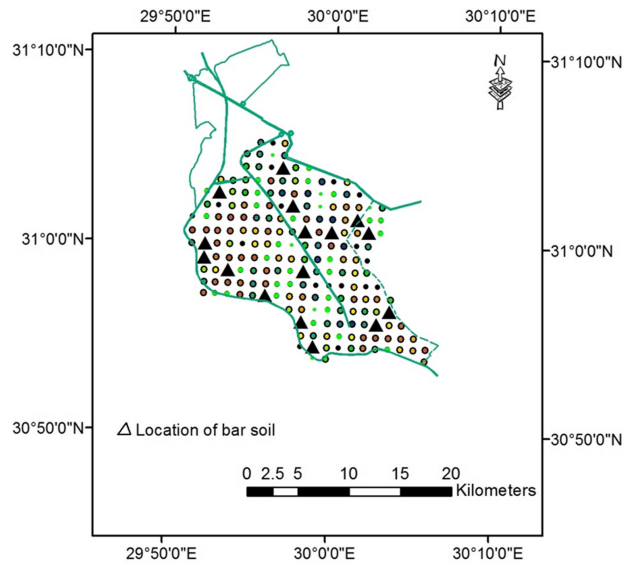


3.2. Processing of the image (stage 2)

After obtaining the corrected Landsat image, the seven spectral SIs in Table 3 were generated using ERDAS spatial modular.

Normalized difference vegetation index (NDVI) shown in Fig. 6 was generated. Soil-adjusted vegetation index (SAVI) was not used as it is not desirable when the study area has sparse vegetation (Ren et al. 2018). NDVI was used to filter the data, which represents bare soil, as when NDVI equals the range between 0.14 and 0.18, it describes the bar soil (Akbar et al. 2019). So only 16 points were used, and the result is shown in Fig. 7.

Figure 7. Bare soil locations using ARCGIS, projected to WGS84 and UTM coordinate system. [Colour online.]



The filtered data for bare soil augers were compared with the pixel value of the seven spectral SIs, which achieved a good correlation in a study area with the same climate conditions in the Al-Behira governorate in Egypt (Abdelaty and Aboukila 2017). There is a correlation between SIs, digital number and EC of the soil (Alavi Panah and Goossens 2001; Abbas and Khan 2007; Tran et al. 2018). So the assessment of the spectral SIs was made to find the best representative SI for the aimed study area.

3.3. Postprocessing (stage 3)

SIs images as shown in Fig. 8 were produced, and their pixel values were extracted to compare them with the field truth data of EC at the specified points. The corresponding pixel value of each point of bare soil was extracted, the correlation between each SI and field data was statically analyzed, and then the coefficient of determination (R^2) for each salinity using simple linear regression was calculated to determine the best representative index as shown in Fig. 9 and Table 4.

4. Discussion and results

For filtration NDVI was used due to its accuracy and simplicity in application (Akbar et al. 2019). There is a high correlation between the reflectance of the soil and its properties such as the content of moisture, soil minerals composition, soil color, and the content of salt (Abdou et al. 2008) that was proved as the results obtained by using regression analysis allowed determining the most correlated and uncorrelated indices with the measured EC. Results of correlation showed that SI5, SI4, and normalized difference salinity index (NDSI) had an acceptable correlation with the field truth data of soil salinity. This finding concurs with the results acquired by Saleh et al. 2017, Allbed et al. 2014, Yossif 2017, Abdelfattah 2009, Pikha 2008, among others. They found that SIs strongly correlated with field soil salinity. Spectral $SI5 = \frac{R \times NIR}{G}$, in which R is red band, NIR is near infrared band, and G is green band, had the best correlation with field measurements = 0.87, highest R^2 , and lowest mean relative error compared to other remaining SIs as shown in Fig. 10 and Table 5.

Figure 8. Images of salinity using ARCGIS, projected to WGS84 and UTM coordinate system. [Colour online.]

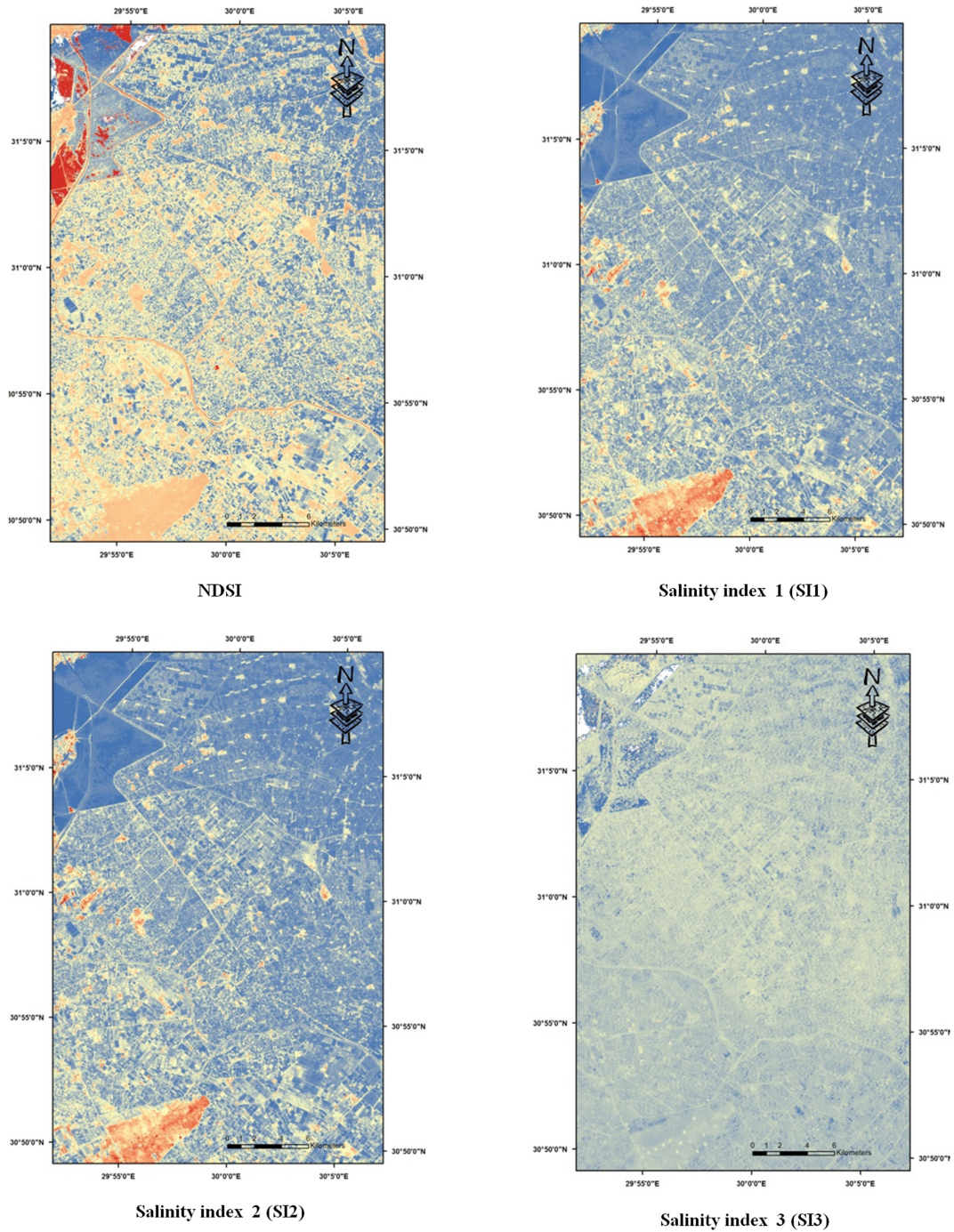


Figure 8. (Continued)

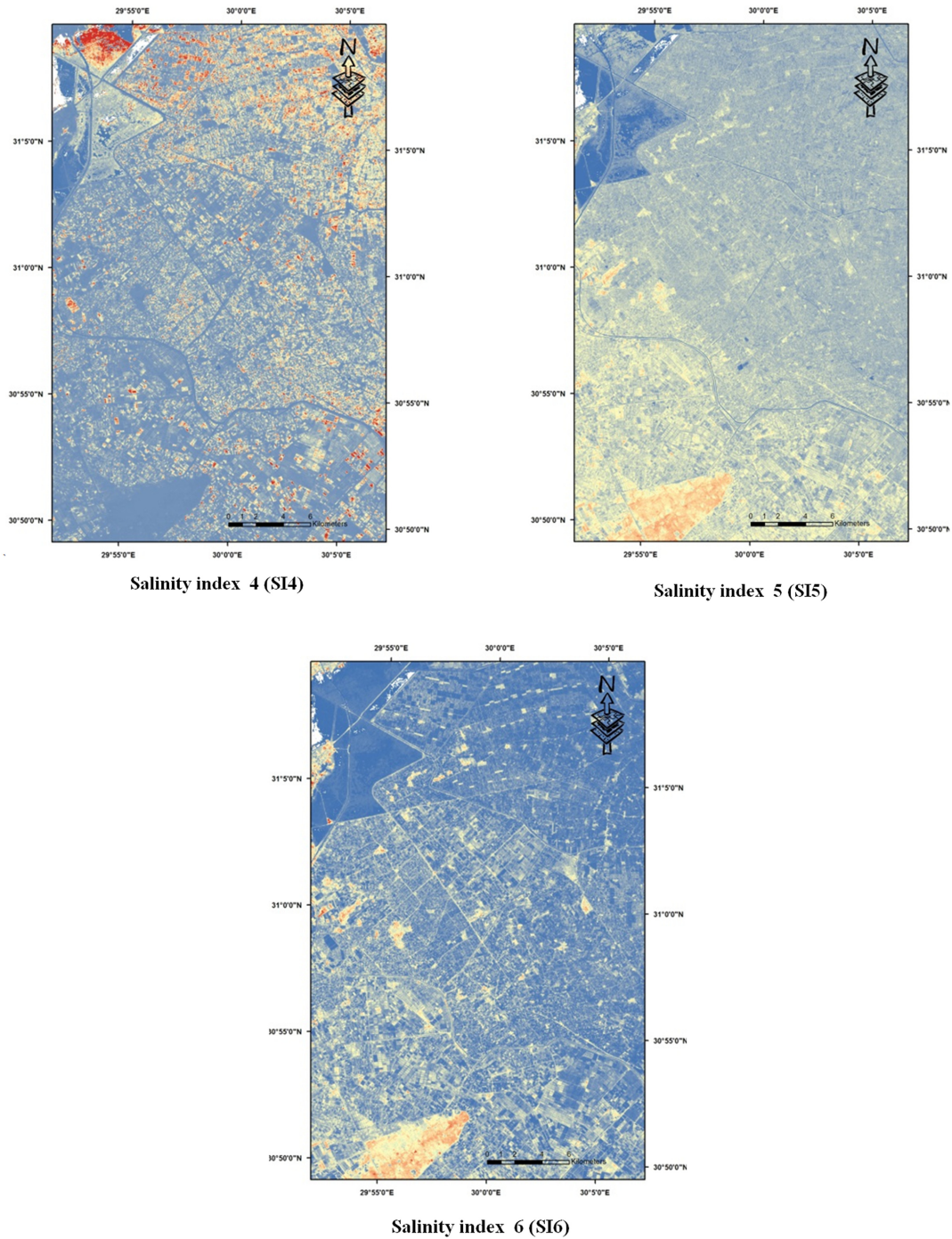


Figure 9. Field salinity versus spectral salinity indices. [Colour online.]

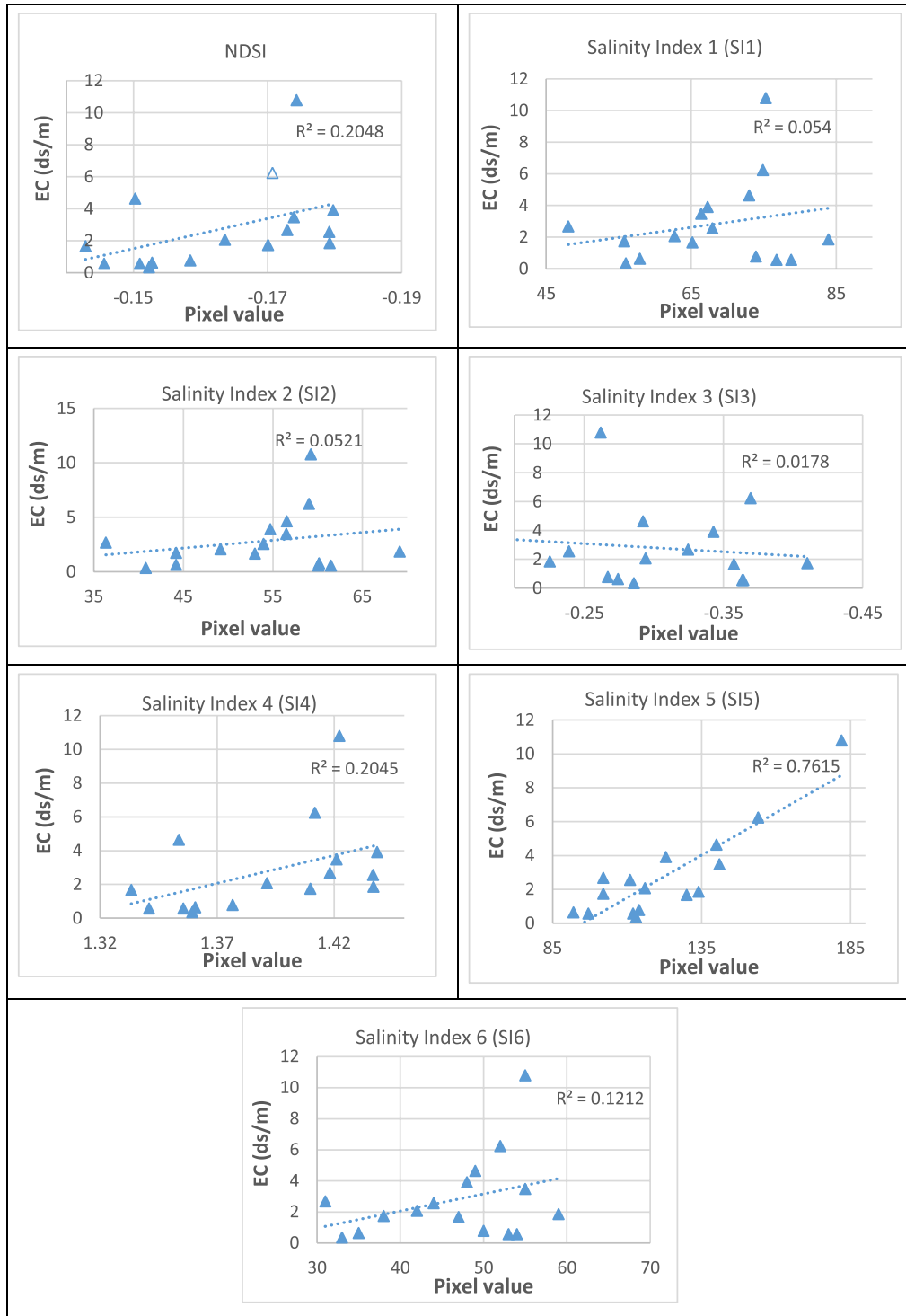
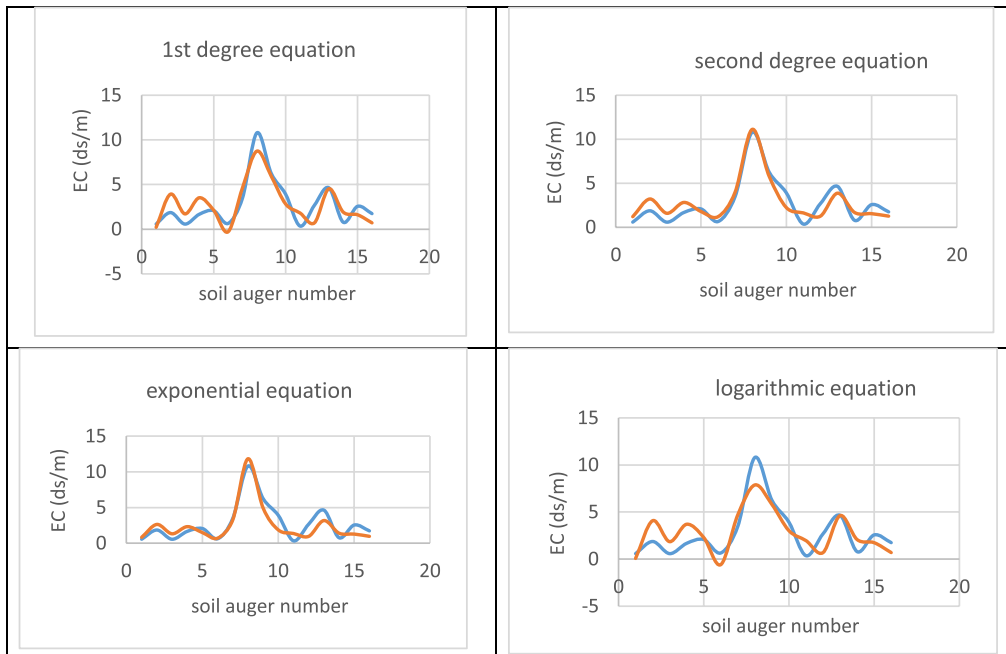


Table 4. Spectral salinity indices correlation and R^2 with field data of electrical conductivity.

Index	Correlation	R^2	Mean relative error (%)
Normalized difference salinity index (NDSI) = $\frac{R-NIR}{R+NIR}$	-0.452	0.205	45.6
Salinity index 1 (SI1) = $\sqrt{G \times R}$	0.232	0.054	87.8
Salinity index 2 (SI2) = $\sqrt{B \times R}$	0.228	0.052	96.9
Salinity index 3 (SI3) = $\frac{B-R}{B+R}$	0.133	0.018	113.6
Salinity index 4 (SI4) = $\frac{NIR}{R}$	0.452	0.204	43.2
Salinity index 5 (SI5) = $\frac{R \times NIR}{G}$	0.870	0.762	22.7
Salinity index 6 (SI6) = $\frac{B \times R}{G}$	0.340	0.121	65.3

Note: B, blue band; G, green band; NIR, near infrared band; R, red band.

Figure 10. Field measurements versus best salinity index using different equations. [Colour online.]**Table 5.** Equations of best index.

Equation	R^2
1st degree equation	0.761
2nd degree equation	0.868
Exponential equation	0.573
Logarithmic equation	0.694

The results showed that using second-degree equation $y = 0.0013x^2 - 0.2459x + 12.809$ has the best as $R^2 = 0.868$ and its graph coincide with the field measurement graph in many points where y values are representing salinity in ds/m and x values are representing the digital number for the point extracted from the best index image.

5. Conclusion

Mapping and monitoring soils affected by salinity are very difficult to study because salinization is a dynamic process. Yet, this research was conducted to assess the spatial soil salinity in the east of the Nile Delta due to its effects on soil, water resource quality, crop production, and infrastructure. Remote sensing has been used for its synoptic coverage and the sensitivity of electromagnetic signals to surface soil parameters such as salinity. The correlation between measured soil salinity and SIs adopted in this research showed that SI5, SI4, and NDSI in sequence had the best significant correlation and R^2 but that SI5 significantly had the best correlation = 0.87 and $R^2 = 0.76$. However these indices may be unsuited for other study regions as their performance varies with many environmental conditions. That approach can lead to map soil salinity without traditional field measurements at low cost and in less time. So it is recommended for decision-makers to use remote sensing techniques to develop effective programs and solutions to reduce or prevent increases in soil salinity in the future.

Author contribution statement

MME-SG: data curation, formal analysis, software, methodology, validation, and original draft writing); MHAM: investigation, supervision, visualization, and writing – review & editing; MRM: conceptualization, resources, and project administration.

Competing interests

The authors declare there are no competing interests.

Data availability

This manuscript does not report data.

Funding

The authors declare no specific funding for this work.

References

- Abbas, A., and Khan, S. 2007. Using remote sensing techniques for appraisal of irrigated soil salinity. MODSIM07 - Land, Water and Environmental Management: Integrated Systems for Sustainability, Proceedings, no. January 2007. pp. 2632–2638.
- Abdelaty, E.F., and Farouk Aboukila, E. 2017. Detection of soil salinity for bare and cultivated lands using Landsat ETM+ imagery data: a case study from El-Beheira governorate, Egypt. Alex. Sci. Exch. J.: Inter. Quarter. J. Sci. Agri. Env. **38** (July–September): 642–653. doi:[10.21608/asejaiqsae.2017.4055](https://doi.org/10.21608/asejaiqsae.2017.4055).
- Abdelfattah, M.A. 2009. Soil salinity mapping model developed using RS and GIS - A case study from Abu Dhabi, United Arab Emirates. Europ. J. Scientif. Res. **26** (3): 342–51. doi:[10.1016/S0167-4889\(01\)00072-6](https://doi.org/10.1016/S0167-4889(01)00072-6).
- Abdou, B., Guedon, A., El Harti, A., Cherkaoui, F., and Ghmari, A. 2008. Characterization of slightly and moderately saline and sodic soils in irrigated agricultural land using simulated data of advanced land imaging (EO-1) sensor. Commun. Soil. Sci. Plant Anal., **39**(November): 2795–2811. doi:[10.1080/00103620802432717](https://doi.org/10.1080/00103620802432717).
- Ahmad, A., Mohd Mawardy, A., Shaun, Q., Suliadi Firdaus, S., and Hamzah, S. 2019. Haze effects on satellite remote sensing imagery and their corrections. Inter. J. Adv. Comp. Sci. Appl. **10** (10): 69–76. doi:[10.14569/ijacsa.2019.0101011](https://doi.org/10.14569/ijacsa.2019.0101011).
- Akbar, T.A., Hassan, Q.K., Sana Ishaq, M.B., Butt, H.J., and Jabbar, H. 2019. Investigative spatial distribution and modelling of existing and future urban land changes and its impact on urbanization and economy. Rem. Sens. **11** (2). doi:[10.3390/rs11020105](https://doi.org/10.3390/rs11020105).
- Alavi Panah, S.K., and Goossens, R. 2001. Relationship between the Landsat TM, MSS DATA and soil salinity. J. Agri. Sci. Technol. **3**: 101–11.

- Allbed, A., Kumar, L., and Sinha, P. 2014. Mapping and modelling spatial variation in soil salinity in the Al Hassa Oasis based on remote sensing indicators and regression techniques. *Rem. Sens.* **6** (2): 1137–1157. doi:[10.3390/rs6021137](https://doi.org/10.3390/rs6021137).
- Amal, M.A., and Benni, J.T. 2010. Monitoring and evaluation of soil salinity in term of spectral response using Landsat images and GIS in Mesopotamian Plain. *J. Iraqi Desert Stud. Special Issue 1st Scient. Conf.* **2**(2): 19–32.
- Asfaw, E., Suryabhagavan, K.V., and Argaw, M. 2018. Soil salinity modeling and mapping using remote sensing and GIS: The case of Wonji Sugar Cane Irrigation Farm, Ethiopia. *J. Saudi Soc. Agri. Sci.* **17** (3): 250–258. doi:[10.1016/j.jssas.2016.05.003](https://doi.org/10.1016/j.jssas.2016.05.003).
- Bannari, A., Guedon, A.M., El-Harti, A., Cherkaoui, F.Z., and El-Ghmari, A. 2008. Characterization of slightly and moderately saline and sodic soils in irrigated agricultural land using simulated data of advanced land imaging (EO-1) sensor. *Commun. Soil Sci. Plant Anal.* **39** (19–20): 2795–2811. doi:[10.1080/00103620802432717](https://doi.org/10.1080/00103620802432717).
- Bannari, A., Nadir Hameid, A.E.-B., and Tashtoush, F. 2017. Salt-affected soil mapping in an arid environment using semi-empirical model and Landsat-Oli data. *Adv. Rem. Sens.* **6** (4): 260–291. doi:[10.4236/ars.2017.64019](https://doi.org/10.4236/ars.2017.64019).
- Brown, J.W., Hayward, H.E., Richards, A., Bernstein, L., Hatcher, J.T., Reeve, R.C., and Richards, L.A. 1954. Diagnosis and improvement of saline and alkali soils. United States Department of Agriculture, Agriculture Handbook.
- El-Dein, A.A.S., and Galal, M.E. 2017. Prediction of reclamation processes in some saline soils of Egypt. **57**(3): 293–301.
- Douaoui, A.E.K., Nicolas, H., and Walter, C. 2006. Soil and remote-sensing data detecting salinity hazards within a semiarid context by means of combining soil and remote-sensing data, no. August 2018. *Geoderma*, **134**(1–2): 217–230. doi:[10.1016/j.geoderma.2005.10.009](https://doi.org/10.1016/j.geoderma.2005.10.009).
- Findings, Experiment. 2013. A Review on Noise Removal Techniques from RemoteSensingImages, no.January. doi:[10.13140/RG.2.1.1104.6168](https://doi.org/10.13140/RG.2.1.1104.6168).
- Fuyi, T., Mohammed, S.K., Abdullah K., Lim, H.S., and Ishola, K.S. 2013. A comparison of atmospheric correction techniques for environmental applications. *International Conference on Space Science and Communication, IconSpace*, no. July: 233–237. doi:[10.1109/IconSpace.2013.6599471](https://doi.org/10.1109/IconSpace.2013.6599471).
- Hammam, A.A., and Mohamed, E.S. 2020. Mapping soil salinity in the east Nile Delta using several methodological approaches of salinity assessment. *Egypt. J. Remote Sens. Space. Sci.* **23** (2): 125–131. doi:[10.1016/j.ejrs.2018.11.002](https://doi.org/10.1016/j.ejrs.2018.11.002).
- Japan International Cooperation Agency. 1995. El-Omoum Main Drainage Improvement report. Al-Behira.
- Khan, N.M., Rastoskuev, V.V., Shalina, E.V., and Sato, Y. 2001. Mapping salt-affected soils using remote sensing indicators-a simple approach with the use of GIS IDRISI. *22nd Asian Conference on Remote Sensing*, 5(9).
- Major, D., Baret, F., and Guyot, G. 1990. A ratio vegetation index adjusted for soil brightness. *Int. J. Remote Sens.* **11**: 727–740. doi:[10.1080/01431169008955053](https://doi.org/10.1080/01431169008955053).
- Metternicht, Z.A.J. 2008. Soil salinity and salinization hazard. In: *Remote sensing of soil salinization*. CRC Press, Boca Raton. doi:[10.1201/9781420065039.pt1](https://doi.org/10.1201/9781420065039.pt1)
- Mohamed, E.S., Morgun, E.G., and Bothina, S.G. 2011. Assessment of soil salinity in the Eastern Nile Delta (Egypt) using geoinformation techniques. *Mosc. Univ. Soil Sci. Bull.* **66**: 11–14. doi:[10.3103/S0147687411010030](https://doi.org/10.3103/S0147687411010030).
- Morshed, M.M., Islam, M.T., and Jamil, R. 2016. Soil salinity detection from satellite image analysis: an integrated approach of salinity indices and field data. *Environ. Monit. Assess.* **188**: 119. doi:[10.1007/s10661-015-5045-x](https://doi.org/10.1007/s10661-015-5045-x). PMID: 26815557.
- Pikha S.D. 2008. Chapter 13. Mapping salinity hazard: an integrated application of remote sensing and modeling-based techniques. Page 257 in G. Metternicht, J.A. Zinck, eds. *Remote Sensing of Soil Salinization: Impact on Land Management*. CRC Press, Boca Raton. doi:[10.1201/9781420065039.pt3](https://doi.org/10.1201/9781420065039.pt3).
- Ren, H., Zhou, G., and Zhang, F. 2018. Using negative soil adjustment factor in soil-adjusted vegetation index (SAVI) for above ground living bio mass estimation in arid grass lands. *Rem. Sens. Environ.* **209**: 439–445. doi:[10.1016/j.rse.2018.02.068](https://doi.org/10.1016/j.rse.2018.02.068).
- Saleh, A M, Belal, A.B., and Mohamed, E.S. 2017. Mapping of soil salinity using electromagnetic induction: A case study of east Nile Delta, Egypt. *Egypt. J. Soil Sci.* **57** (2): 167–174. doi:[10.21608/ejss.2017.3705](https://doi.org/10.21608/ejss.2017.3705).
- Schneier-Madanes, G., and Courel, M.-F. 2010. *Water and Sustainability in Arid Regions: Bridging the Gap Between Physical and Social Science*. doi:[10.1007/978-90-481-2776-4](https://doi.org/10.1007/978-90-481-2776-4).
- Shahid, S.A., Abdelfattah, M.A., and Taha, F.K. 2013. *Developments in Soil Salinity Assessment and Reclamation, Innovative Thinking and Use of Marginal Soil and Water Resources in Irrigated Agriculture*; Springer Science + Business Media, B.V.: Berlin, Germany. p. 808. ISBN 978-94-007-5684-7
- Tran, P.H., Ywei-an Liou, A.K.N., Phi Hoang, P., and Thanh, H. 2018. Estimation of Salinity Intrusion by Using Landsat 8 OLI Data in The Mekong Delta Progress. *Earth and Planetary Science journal*. doi:[10.20944/preprints201808.0301.v1](https://doi.org/10.20944/preprints201808.0301.v1).
- Yossif, M.H. 2017. Change detection of land cover and salt affected soils at Siwa Oasis, Egypt. *Alex. Sci. Exch. J.: Inter. Quarter. J. Sci. Agri. Environ.* **38** (July-September):44662. doi:[10.21608/asejaiqsae.2017.3747](https://doi.org/10.21608/asejaiqsae.2017.3747).